Accepted Manuscript

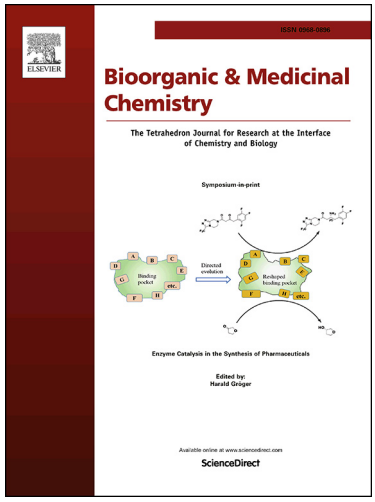

Discovery and Evaluation of nNa$_v$1.5 Sodium Channel Blockers with Potent Cell Invasion Inhibitory Activity in Breast Cancer Cells

Shilpa Dutta, Osbaldo Lopez Charcas, Samuel Tanner, Frédéric Gradek, Virginie Driffort, Sébastien Roger, Katri Selander, Sadanandan E. Velu, Wayne Brouillette

PII: S0968-0896(17)32218-6
DOI: https://doi.org/10.1016/j.bmc.2018.04.003
Reference: BMC 14286

To appear in: *Bioorganic & Medicinal Chemistry*

Received Date: 20 November 2017
Revised Date: 25 March 2018
Accepted Date: 1 April 2018

Please cite this article as: Dutta, S., Lopez Charcas, O., Tanner, S., Gradek, F., Driffort, V., Roger, S., Selander, K., Velu, S.E., Brouillette, W., Discovery and Evaluation of nNa$_v$1.5 Sodium Channel Blockers with Potent Cell Invasion Inhibitory Activity in Breast Cancer Cells, *Bioorganic & Medicinal Chemistry* (2018), doi: https://doi.org/10.1016/j.bmc.2018.04.003

Discovery and Evaluation of nNa$_v$1.5 Sodium Channel Blockers with Potent Cell Invasion Inhibitory Activity in Breast Cancer Cells

Shilpa Dutta[1,2], Osbaldo Lopez Charcas[3], Samuel Tanner[1,2], Frédéric Gradek[3], Virginie Driffort[3], Sébastien Roger[3,4], Katri Selander[5], Sadanandan E. Velu[1,2]* and Wayne Brouillette[1,2]*

[1]Department of Chemistry, University of Alabama at Birmingham, 901 14th Street South, Birmingham, AL 35294-1240, USA

[2]Center for Biophysical Sciences and Engineering, University of Alabama at Birmingham, 1025 18th Street South, Birmingham, AL 35294-1240, USA

[3]Inserm UMR1069, Nutrition, Croissance et Cancer, Université de Tours, Faculté de médecine, 10 Boulevard Tonnellé, 37032 Tours, Cedex, France

[4]Institut Universitaire de France, 1, rue Descartes, 75231 Paris Cedex 05, France

[5]Division of Hematology and Oncology, Department of Medicine, University of Alabama at Birmingham, 1808 7th Ave S, Birmingham, AL 35294-0012, USA

*Co-corresponding authors: Phone: (205) 934 4747 (Brouillette); Fax: (205) 934-2543; Email: wbrou@uab.edu; Phone: (205) 975 2478 (Velu); Fax: (205) 934-2543; Email: svelu@uab.edu

Abstract:

Voltage-gated sodium channels (VGSC) are a well-established drug target for anti-epileptic, anti-arrhythmic and pain medications due to their presence and important roles that they play in excitable cells. Recently, their presence has been recognized in non-excitable cells such as cancer cells and their overexpression has been shown to be associated with metastatic behavior in a variety of human cancers. The neonatal isoform of the VGSC subtype, $Na_v1.5$ ($nNa_v1.5$) is overexpressed in the highly aggressive human breast cancer cell line, MDA-MB-231. The activity of $nNa_v1.5$ is known to promote the breast cancer cell invasion *in vitro* and metastasis *in vivo*, and its expression in primary mammary tumors has been associated with metastasis and patient death. Metastasis development is responsible for the high mortality of breast cancer and currently there is no treatment available to specifically prevent or inhibit breast cancer metastasis. In the present study, a 3D-QSAR model is used to assist the development of low micromolar small molecule VGSC blockers. Using this model we have designed, synthesized and evaluated five small molecule compounds as blockers of $nNa_v1.5$-dependent inward currents in whole-cell patch-clamp experiments in MDA-MB-231 cells. The most active compound identified from these studies blocked sodium currents by 34.9 ± 6.6 % at 1 μM. This compound also inhibited the invasion of MDA-MB-231 cells by 30.3 ± 4.5 % at 1 μM concentration without affecting the cell viability. The potent small molecule compounds presented here have the potential to be developed as drugs for breast cancer metastasis treatment.

Key Words: Breast cancer, $nNa_v1.5$, voltage-gated sodium channel, sodium current, cancer cell invasion, metastasis.

List of abbreviations:

$CDCl_3$	Deuterated chloroform
CH_2Cl_2	Methylene dichloride
^{13}C-NMR	Carbon-13 nuclear magnetic resonance
CoMFA	Comparative molecular field analysis
$CuBr.Me_2S$	Copper bromide dimethyl sulfide
DMEM	Dulbecco's modified eagle medium
DMSO	Dimethyl sulfoxide
3D-QSAR	3-Dimensional quantitative structure activity relationship
Et_3N	Triethylamine
EtOAc	Ethyl acetate
ER	Estrogen receptor
FBS	fetal bovine serum
HER-2	Human epidermal growth receptor 2
^{1}H-NMR	Hydrogen-1 nuclear magnetic resonance
IC_{50}	Inhibition concentration at 50%
I_{Na}	Sodium currents
MeOH	Methanol
MTS	[3-(4,5-Dimethylthiazol-2-yl)-5-(3-carboxymethoxyphenyl)-2-(4-sulfophenyl)-2H-tetrazolium]

$NaBH(OAc)_3$	Sodium triacetoxyborohydride
$nNa_v1.5$	Neonatal $Na_v1.5$ isoform
Na_2SO_4	Sodium sulfate
NH_3	Ammonia
NHE1	Na+/H+ exchanger type 1
NMR	Nuclear magnetic resonance
PBS	Phosphate buffered saline
pHi	Intracellular pH
ppm	Parts per million
PR	Progesterone receptor
PSS	Physiological saline solution
Rf	Retention factor
THF	Tetrahydrofuran
TMS	Tetramethylsilane
TLC	Thin layer chromatography
TTX	Tetrodotoxin
UV	Ultraviolet
VGSC	Voltage-gated sodium channels

1. Introduction

Despite the increased awareness and advances in treatment, breast cancer remains as the leading cause of cancer death in women.[1-2] Though the survival rate for patients diagnosed with localized breast cancer has improved significantly, it is the metastatic form of the disease that is mainly associated with mortality.[3-4] Metastasis development has a complex mechanism which involves the acquisition of the ability by cancer cells to degrade and migrate through extracellular matrices (ECM) to distant tissues.[5-7] The biggest hurdle in controlling breast cancer associated mortality is the lack of proper treatment for metastasis targeting and prevention.[8-9] Thus, there is an urgent need to identify new druggable therapeutic targets for the treatment and prevention of breast cancer metastasis. One such promising anti-metastasis drug target is the voltage-gated sodium channels (VGSC).[10-14] VGSCs have long been identified and characterized in excitable cells in which they are responsible for the initiation and propagation of action potentials.[15-16] In recent years, VGSC expression has been found to be profoundly and aberrantly enhanced in some non-excitable cells, including a variety of aggressive human cancers of epithelial origin such as lung, prostate, ovarian, colon and breast cancer, and this overexpression is associated with cancer cell invasiveness.[11, 17-22] Voltage-gated sodium channels are abnormally expressed in tumors, often as neonatal isoforms.[23] These channels are not expressed in the non-aggressive cancer cells or normal tissue, providing selectivity in targeting metastatic cancer cells. Their expression levels and activities are related to the aggressiveness of the metastatic form of the cancer giving us the prospect of developing drugs that could specifically inhibit the neonatal VGSC leaving the adult isoform fully functional in the excitable cells.[15]

Nine different VGSC isoforms have been identified, and are classified as $Na_v1.1$-$Na_v1.9$.[24-25] The major VGSC isoform expressed in aggressive tumor biopsies and metastatic

breast cancer cells, such as triple-negative [estrogen receptors (ER-), progesterone receptor (PR-), human epidermal growth receptor 2 (HER-2-)] MDA-MB-231 cells,[22] is $nNa_v1.5$, a neonatal splice variant showing a substitution of seven amino acids in the first domain of the channel compared to the adult isoform.[26] In a normal scenario, VGSCs open and inactivate within a few milliseconds under membrane depolarization but in cancer cells $nNa_v1.5$ remains in a partially activated and non-inactivated state at the resting membrane potential of cells (around -40mV, because of a window of voltage between -60 and -20 mV), resulting in a continuous inward flow of Na^+ ions (called window current).[22] Literature reports strongly support the involvement of VGSC in breast cancer cell invasiveness; where overexpression of nNav1.5 (*SCN5A gene*) and low expression of auxiliary β4-subunit (*SCN4B gene*) promote the development of metastasis.[10, 27-29] Metastasis development depends on numerous abilities acquired by highly aggressive cancer cells, one of which is their ability to degrade ECM mediated by various extracellular proteases such as matrix metalloproteinases and cysteine cathepsins.[30-32] Investigations on the mechanistic role of $nNa_v1.5$ in metastasis revealed that $nNa_v1.5$ along with the Na^+/H^+ exchanger type 1 (NHE1) and caveolin-1 are all colocalized in the invasive structures of MDA-MB-231 cells, called invadopodia.[28] NHE1, often overexpressed and over-activated in breast cancer cells, is the central regulator of intracellular and perimembrane pH augmenting the ECM proteolysis.[33] $nNa_v1.5$ and NHE1 are functionally coupled to enhance H^+ efflux, acidifying the extracellular pH.[28] The extracellular matrix proteolytic activity in MDA-MB-231 cells is induced by acidic cysteine cathepsins B and S, which are released as soluble proforms in the extracellular microenvironment and are activated in an acidic pH.[27, 31] Thus, nNav1.5 displays a persistent activity at the membrane potential of breast cancer cells, which is responsible for the increased ECM proteolysis and cancer cell invasiveness. Since the functional activity, and not simply the

presence, of $nNa_v1.5$ channels is required to promote breast cancer cell invasiveness, $nNa_v1.5$ constitute a promising target for the breast cancer metastasis drug discovery.[34] It is important to note that numerous clinically used drugs target various subtypes of VGSCs in excitable tissues.[35] These drugs have acceptable toxicity as find use as local anesthetics, antiarrhythmics, anticonvulsants, and for treating neuropathic pain.[36] Similar clinical utility can also be anticipated for $nNa_v1.5$ blockers for the treatment of breast cancer, particularly since nNav1.5 is a neonatal variant not normally found in normal adult tissues.

Designing ligands for VGSCs has been, and continues to be, difficult since detailed structural information of the drug binding site for this integral membrane protein remain largely unclear. In recent years, we have developed a highly predictive, comprehensive 3D-QSAR model for the design of VGSC ligands using Comparative Molecular Field Analysis (CoMFA).[37] This 3D-QSAR model samples the differences in steric and electrostatic fields surrounding each ligand in the training set, in 3D space, and correlates these changes with its biological activity.[38] The training set for this model utilized several classes of drugs targeting sodium channels, including local anesthetics, anticonvulsants and antiarrhythmics.[37] A total of 67 compounds were used to train this comprehensive 3D-QSAR model, which well covered 3D space and spanned over 4 orders of magnitude in biological activity. This model was used to design a large number of new small organic molecules, not yet synthesized or evaluated, with predicted VGSC activities near 100 nM. Several of these were then synthesized and evaluated for VGSC binding activity against a mixed population of VGSCs. Potency predictions by this model have been highly accurate for all compounds that were evaluated. Here we synthesized five compounds (Fig. 1) predicted to have low nanomolar VGSC binding and evaluated these for the inhibition of $nNa_v1.5$ currents and inhibition of invasion using MDA-MB-231 cells.

Figure 1: Compounds evaluated for the inhibition of $nNa_v1.5$ currents in breast cancer MDA-MB-231 cells.

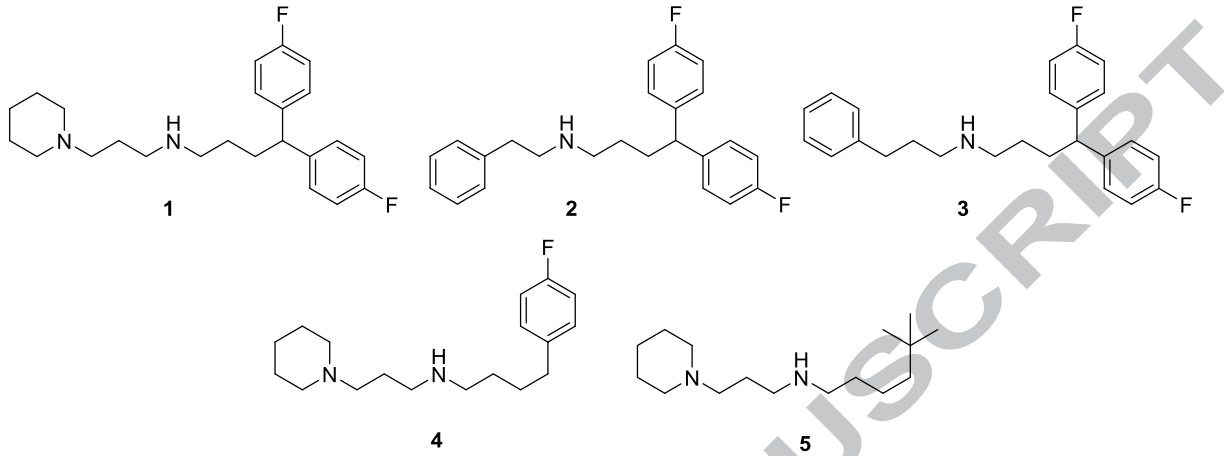

2. Results and Discussion:

2.1. Chemistry:

Two straightforward approaches were employed for the synthesis of the target compounds **1**-**5**. Compounds **1**-**3** were synthesized by *N*-alkylation of the suitable amines by treatment with 4,4-di-(4-fluorophenyl)butyl chloride (**6**) in the presence of Et_3N in DMSO at 80^{o}C for 7-8 h as outlined in Scheme 1. Compound **1** was prepared by alkylation of 3-(*N*-piperidino)propylamine with compound **6** in DMSO in 60% yield. Alkylation of 2-phenethylamine with compound **6** yielded compound **2** in 58% yield and a similar alkylation of 3-phenylpropylamine with compound **6** afforded the target compound **3** in 60% yield.

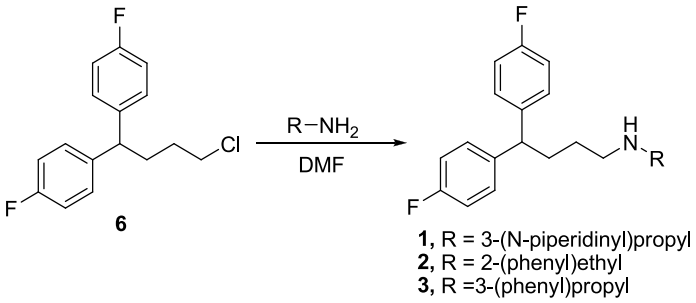

Scheme 1: Synthesis of compounds **1**, **2** and **3**.

Compounds **4** and **5** were synthesized via a reductive amination procedure as outlined in Schemes 2 and 3, respectively. The synthesis of compound **4** began with the reduction of 4-(4-fluorophenyl)-4-oxobutanoic acid (**7**) using borane / *tert*-butylamine complex and $AlCl_3$ in anhydrous CH_2Cl_2 resulting in the formation of 4-(4-fluorophenyl)butan-1-ol (**8**) in 50% yield. Compound **8** was oxidized with PCC in CH_2Cl_2 to furnish 4-(4-fluorophenyl)butan-1-al (**9**) in 52% yield.[39] The aldehyde (**9**) was then subjected to reductive amination using 3-(*N*-piperdino)propylamine in the presence of $NaBH(OAc)_3$ in anhydrous CH_2Cl_2 resulting in the formation of compound **4** in 30% yield.

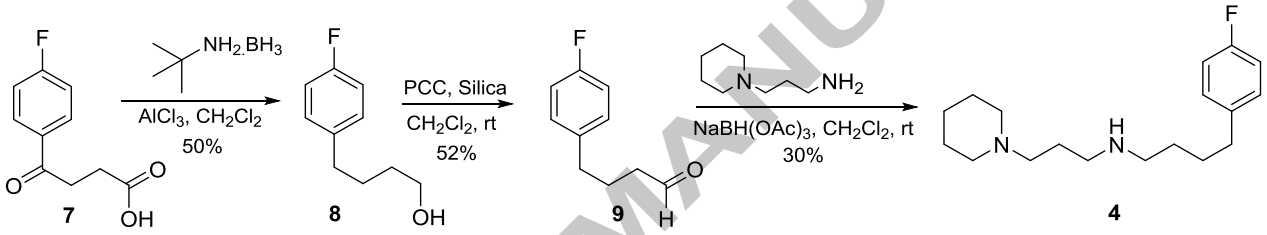

Scheme 2: Synthesis of compound **4**

The synthesis of compound **5** started with the preparation of the Grignard reagent **11** by refluxing a solution of neopentyl bromide (**10**) in anhydrous THF with Mg metal in the presence of iodine. The resulting neopentyl magnesium bromide was reacted with acrolein via Michael addition using CuBr-Me_2S, TMSCl, and HMPA in anhydrous THF at -100^oC to provide (5,5-dimethylhex-1-enyloxy)trimethylsilane (**12**) with 61% yield.[40] The next two steps, removal of the TMS group from compound **12** and the reductive amination were carried out as a one pot due to the instability of the intermediate aldehyde, 5,5-dimethylhexanal (**13**). The TMS group was removed by stirring the compound **12** with KF in MeOH at 0^oC, and the aldehyde **13** thus obtained was reacted with 3-(*N*-piperidino)propylamine in MeOH in the presence of $NaBH(OAc)_3$ to afford the compound **5** in 50% yield.

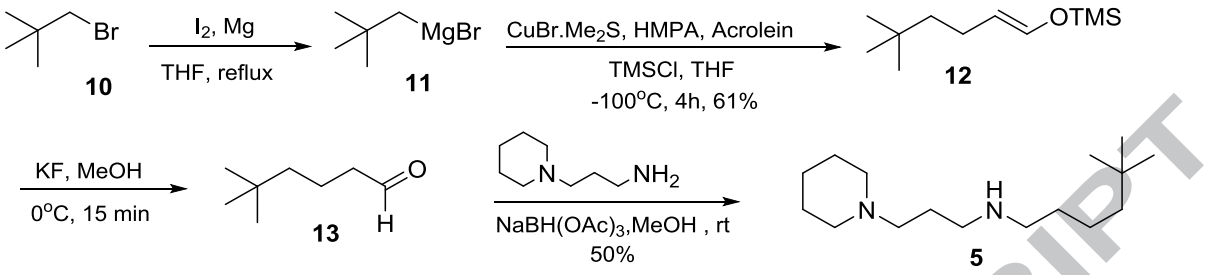

Scheme 3: Synthesis of compound **5**

2.2. Biological evaluation:

The mechanistic studies so far on the involvement of $nNa_v1.5$ in breast cancer progression reveal that they promote cell invasion without playing any role in cell proliferation. Therefore, the cytotoxicity of compounds was first evaluated to avoid misinterpretation of the effects of compounds on invasion or channel currents. Cell viability was evaluated using a colorimetric MTS assay. All the biological evaluations were carried out using the highly aggressive human breast cancer cell line, MDA-MB-231. Compounds were tested at a range of concentrations from 1.0 to 25 μM, as compared to a control containing no drug. All solutions contained 2% PBS and 0.2% DMSO. Cell viability was assessed after 24 hours of drug treatment. Maximum non-toxic concentrations were determined for each compound and none of the compounds affected cell viability at concentrations <5 μM (Table 1). Compound **1** displayed a maximum non-toxic concentration of 5 μM while compound **4** displayed least cytotoxicity with a maximum non-toxic concentration of 25 μM. Maximum non-toxic concentrations for compounds 2, 3 and 5 were found to be about 10 μM. For compounds **1** and **4**, these values are much higher than the concentrations required (0.1 μM and 1 μM) to produce significant nNav1.5 current blockade and cell invasion inhibition (Table 1, Figs. 2A and 3A).

Table 1: Cell viability, $nNa_v1.5$ current blockade and invasion inhibition of compounds **1-5** in MDA-MB-231 cells

Compd No	Maximum nontoxic concentration[a]	% Blockade of I_{Na} peak currents[b]	% Inhibition of cell invasion[c]
1	5 μM	34.9 ± 6.6 % at 1 μM (n = 6)	30.3 ± 4.5 % at 1 μM
2	10 μM	~ 30 % at 10 μM (n = 2)	NE[e]
3	10 μM	~ 30 % at 10 μM (n = 2)	NE[e]
4	>25 μM [d]	25.0 ± 3.3 % at 1 μM (n = 21)	28.0 ± 5.7 % at 1 μM
5	10 μM	~30 % at 10 μM (n = 2)	NE[e]
TTX [22]	30 μM	> 95%	31.5 ± 3.8 % at 30 μM

a. Determined by five measurements, b. Evaluated in 'n' cells and expressed as mean ± SEM, c. Average of seven repeats, expressed as mean ± SEM, d. Maximum concentration tested, e. Not evaluated.

The inhibition of sodium currents (I_{Na} inhibition) in individual MDA-MB-231 cells by compounds at 10 μM concentration was initially measured in physiological saline solution (PSS) using whole-cell patch-clamp experiments conducted according to a reported protocol.[27] In this study, cells were continuously perifused with PSS control solution (containing the same percentage of DMSO, as used in the solvent for the test compounds) or the test compounds. After 5-10 min perifusion of the compounds, depolarization steps and I_{Na}-V protocols were run. At 10 μM, all five compounds showed some reduction in peak sodium currents. Compounds **1** and **4** were most active exhibiting 50 % and 60 % I_{Na} inhibition at 10 μM concentration, while compounds **2, 3** and **5** showed relatively less I_{Na} inhibition of ~30% (Table 1 and Figs. 2A and 3A). As the compounds **1** and **4** were better blockers, they were further evaluated at a range of concentrations from 0.1 μM to 100 μM to examine the dose response relationship on I_{Na} inhibition as well as to determine the IC_{50} values. Results of these studies are summarized in Figs. 2 and 3.

Both compounds **1** and **4** demonstrated a slow, dose-dependent inhibition of the maximal current elicited for a membrane depolarization from -100 to -5 mV, which was not reversible (for compound **1**) or weakly reversible (for compound **4**) after wash-out (Figs. 2B and 3B). Compound **1** exhibited an IC_{50} value of 4.8 ± 1.2 µM (n = 3-6 cells)whereas compound **4** exhibited an IC_{50} value of 5.9 ± 0.9 µM (n = 17-21 cells), (Figs. 2C and 3C, respectively). In addition, the effect of the two compounds was studied on the activation and inactivation kinetics of the sodium current (Figs. 2D and 3D). Indeed, compound **1** (at 10 µM) significantly slowed down both activation and inactivation kinetics of I_{Na} measured for a membrane depolarization from -100 to -5 mV (Figs. 2A and 2D), while compound **4** only reduced kinetics of activation (Figs. 3A and 3D). The effect of Compounds **1** and **4** tested at a concentration of 10 µM on the full I_{Na}-Voltage relationship (from -100 to +60 mV) is shown in figures 2E and 3E, respectively. The voltage of half-inactivation ($V_{1/2}$-inactivation) significantly shifted to hyperpolarized values from –71.6 ± 0.4 mV in control condition, to –88.6 ± 3.4 mV in presence of compound **1** (n = 6 cells, $p<0.01$, Fig. 2F), while half-voltage of activation ($V_{1/2}$-activation) was unchanged. Compound **4** also shifted $V_{1/2}$-inactivation to hyperpolarized values from –66.0 ± 2.5 mV (in control condition) to –77.5 ± 3.0 mV (n= 15 cells, $p<0.01$, Fig. 3F). In addition, compound **4** also showed a light hyperpolarizing shift in $V_{1/2}$-activation from –30.7 ± 0.9 mV (in control condition) to –36.8 ± 2.8 mV (n = 15 cells, $p<0.001$, Fig. 3F).

These results indicate that the lead compounds **1** and **4** exhibited significant blockade of $nNa_v1.5$ currents in MDA-MB-231 cells in low micromolar concentrations. These effects were observed to be weakly reversible. Furthermore, these two compounds induced significant leftward shift in the inactivation-voltage relationship suggesting that they could also reduce the window of voltage, and therefore reduce the persistent window current associated with cancer

cell invasiveness. The observed nNav1.5 current blockade for compounds **1** and **4** were compared to the positive control tetrodotoxin (TTX), which is a known sodium channel blocker (>95% blockade at 30 μM).[22] Compounds **1** and **4** displayed similar activity to TTX with 25 - 35 % blockade at 1 μM, 50-60% blockade at 10 μM. However, it required about 100 μM of compounds **1** and **4** to produce a >95% blockade of channel current. The observed nNav1.5 current blockade by compounds **1** and **4** are unrelated to any effects on cell viability as their maximum cell cytotoxicity concentrations were much higher at 5 μM and 25 μM respectively. Based on these experimental results, compounds **1** and **4** were selected for further evaluation in cell invasion assays.

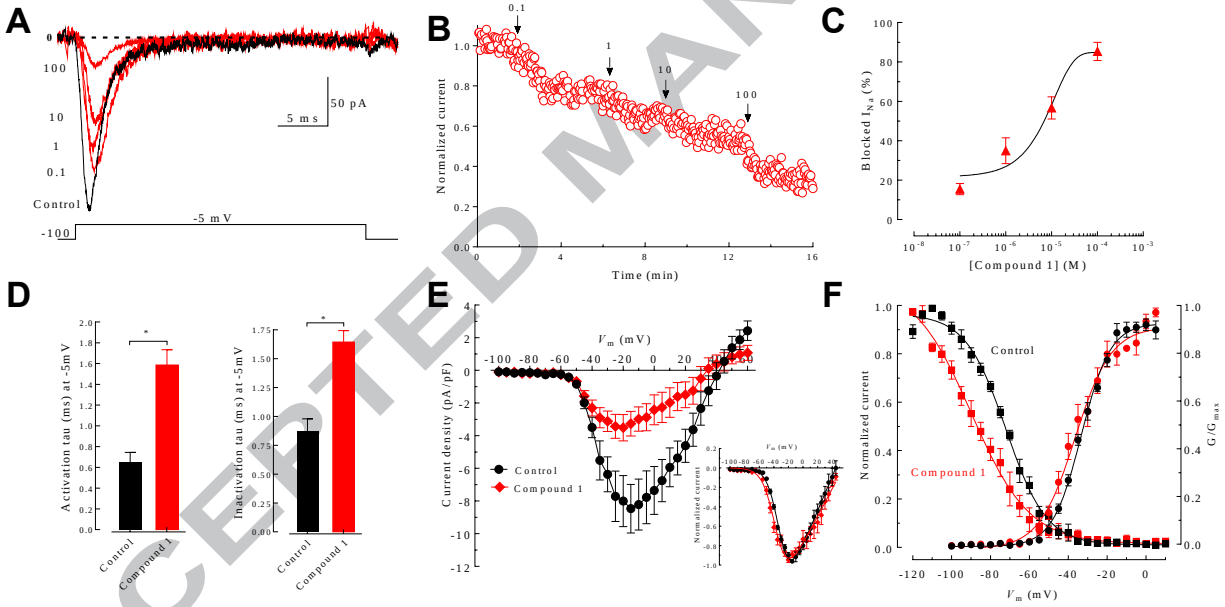

Figure 2: Effects of compound 1 on voltage-gated sodium currents from MDA-MB-231 cells. A) representative recordings showing steady-state block of $Na_V1.5$ currents by increasing concentrations (from 0.1 to 100 μM) of **compound 1**. Whole-cell patch-clamp recordings were obtained in MDA-MB-231 cells and sodium currents were evoked by 30 ms duration voltage steps to ─5 mV from a holding potential of ─100 mV, applied every 2 s. The dotted line represents the zero current level. **B)** Time course of $Na_V1.5$ channels block by **compound 1**. Peak currents generated for a depolarization step from -100 to -5 mV were normalized to control amplitude (before drug exposure), and defined as the fraction of I_{Na} remaining. **C)** Concentration-response relationships for the effect of **compound 1** on $Na_V1.5$ channels. Percent blocked current was calculated from peak current measurements from step voltages from -100 to

–5 mV in the presence of **compound 1** concentrations indicated in the figure. Data from these experiments were fitted using a Hill equation (IC_{50} = 4.8 ± 1.2 µM; Hill's slope = 0.56 ± 0.09). **D) Compound 1** slows down the activation and inactivation kinetics of $Na_V1.5$ currents. Currents like those illustrated in panel A were fitted with two exponentials functions, one for the activation and the other for the inactivation of the current at –5 mV, and the respective time constants (τ) were plotted. Columns, means from six cells before (control) and after a steady-state block (**compound 1**, at 10 µM). *, statistical significance with a Student's t test ($P < 0.05$) represent mean values. **E)** *I-V* curves in absence and presence of 10 µM of **compound 1**. The inset shows the normalized current-voltage relationship obtained from same cells, where values were normalized to the maximal current recorded in each condition. **F)** Activation- of peak Na^+ conductance (filled circles) and steady-state inactivation-voltage relationships (filled squares) of $Na_V1.5$ channels from MDA-MB-231 cells in absence and presence of 10 µM **compound 1**. Smooth lines are fits to Boltzmann functions and $V_{1/2}$ values were calculated for each condition. While the $V_{1/2}$-activation voltage were not significantly different, –33.0 ± 1.2 mV in control condition and to – 34.9 ± 2.8 mV in presence of compound 1, the $V_{1/2}$-inactivation voltage was significantly shifted to hyperpolarized values from – 71.6 ± 0.4 mV in control condition, to – 88.6 ± 3.4 mV in presence of compound 1 (p<0.01, Mann-Whitney Rank Sum test). All data were obtained from 6 cells.

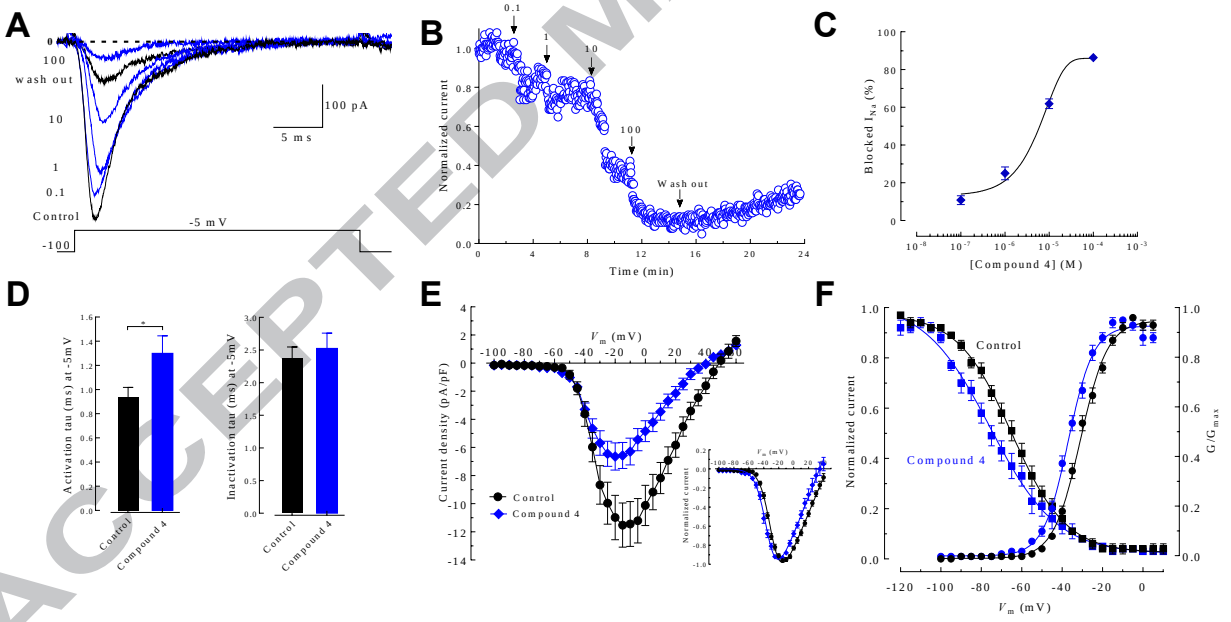

Figure 3: Effects of compound 4 on voltage-gated sodium currents from MDA-MB-231 cells. **A)** Representative recordings showing steady-state block of $Na_V1.5$ currents by increasing concentrations (from 0.1 to 100 µM) of **compound 4.** Whole-cell patch-clamp recordings were obtained in MDA-MB-231 cells and sodium currents were evoked by 30 ms duration voltage steps to –5 mV from a holding potential of –100 mV, applied every 2 s. The dotted line represents the zero current level. **B)** Time course of $Na_V1.5$ channels block by **compound 4**.

Peak currents generated for a depolarization step from -100 to -5 mV were normalized to control amplitude (before drug exposure), and defined as the fraction of I_{Na} remaining, only a slight fraction of the initial current amplitude was recovered after drug washing (17.4 ± 3.1 %). **C)** concentration-response relationships for the effect of **compound 4** on $Na_V1.5$ channels. Percent blocked current was calculated from peak current measurements from step voltages to −5 mV in the presence of increasing concentrations of **compound 4** (n = 22). Data from these experiments were fitted using a Hill equation (IC_{50} = 5.9 ± 0.9 μM; Hill's slope = 0.72 ± 0.06). **D) Compound 4** slows down the activation but not the inactivation kinetics of $Na_V1.5$ currents. Currents like those illustrated in panel A were fitted with two exponentials functions, and the respective time constants (τ) were plotted. Columns, means from 17 cells before (control) and after a steady-state block (**compound 4**, at 10 μM). *, statistical significance with a Student's t test ($P < 0.05$). **E)** *I-V* curves in absence and presence of 10 μM **compound 4**. The inset shows the normalized current-voltage relationship obtained from same cells, where values were normalized to the maximal current recorded in each condition. **F)** Activation of peak Na^+ conductance (filled circles) and steady-state inactivation (filled squares) of $Na_V1.5$ channels from MDA-MB-231 cells in absence and presence of 10μM **compound 4**. Smooth lines are fits to Boltzmann functions and $V_{1/2}$ values were calculated for each condition. $V_{1/2}$-activation voltage values were significantly different and compound 4 induced a light hyperpolarizing shift from – 30.7± 0.9 mV in control condition to – 36.8 ± 2.8 mV in presence of compound 4 ($p<0.001$, Mann-Whitney Rank Sum test). The $V_{1/2}$-inactivation voltage was also significantly shifted to hyperpolarized values from – 66.0 ± 2.5 mV in control condition, to – 77.5 ± 3.0 mV in presence of compound 4 ($p<0.01$, Mann-Whitney Rank Sum test). These data were obtained from 15 cells.

Compounds **1** and **4** were then evaluated for their ability to inhibit invasion of MDA-MB-231 cells using Matrigel-coated inserts in a trans-well invasion assay.[41] Matrigel (Becton Dickinson matrix) mimics the extracellular matrix and basement membrane that metastatic cells must cross to enter the blood stream and travel to lymph nodes or invade distant organs. The ability of cancer cells to invade is measured based on the number of cells that can invade the matrigel and migrate through the pores across the membrane. The triple negative MDA-MB-231 cell line is one of the most invasive/ metastatic cell lines available to study breast carcinoma. Compounds **1** and **4** were evaluated in the invasion assay at 0.1 μM and 1 μM along with the control compound TTX at 30 μM. The results of the invasion assay are presented in Fig. 4. As

shown, both **1** and **4** exhibited 20% inhibition of invasion at 0.1 μM in comparison to the control, whereas, at 1 μM, both compound **1** and **4** showed a significant reduction of invasion (30%), similar level to what is observed for TTX at 30 μM (Fig. 4 and Table1). These results suggest that our lead compounds **1** and **4** are very effective in inhibiting cell invasion producing an effect similar to TTX at a much lower concentration. Furthermore, the lead compounds **1** and **4** are more drug-like and have simpler chemical structures than TTX. In recent studies, VGSC-blocking antiepileptic drug phenytoin and antiarrhythmic drug ranolazine inhibited the invasion of metastatic MDA-MB-231 cells *in vitro* and reduced breast cancer metastasis *in vivo* without much neuro-muscular or cardiac toxicity demonstrating good therapeutic index.[42-44] Both these drugs (with Na+ current blockade and invasion inhibition at 50 μM) are considerably less active than our lead compounds (Na+ current blockade and invasion inhibition at 1μM) *in vitro*. Therefore, we expect our lead compounds to be more potent *in vivo* and exhibit better therapeutic index than phenytoin and ranolazine.

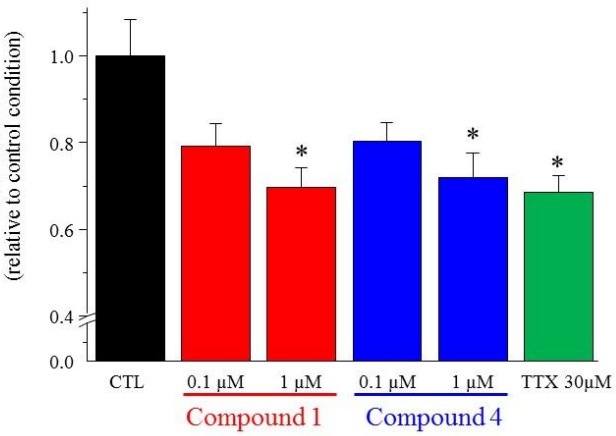

Figure 4: Effects of compounds 1 and 4 on MDA-MB-231 cancer cells invasive properties. Effect of compounds **1** and **4** tested at 0.1 and 1 μM concentrations on MDA-MB-231 human breast cancer cell invasiveness, as compared to the effect of the sodium channel inhibitor tetrodotoxin (TTX, 30 μM). Results were obtained from 7 independent experiments, and are expressed as relative invasion (mean ± SD), normalized to the control condition (CTL) obtained

without drug but with the maximal solvent dose (DMSO 0.2%). *, indicates a statistical difference at $p<0.05$ (Mann-Whitney Rank Sum test).

3. Conclusions:

The presence of $nNa_v1.5$ in aggressive breast cancer cells and their association with invasive behavior is well established. Here, we report the discovery of small, potent drug-like blockers of $nNa_v1.5$ channel. A 3D-QSAR model is used to assist the discovery of low micromolar small molecule $nNa_v1.5$ blockers. Using this model we have designed, synthesized and evaluated five small molecule compounds as blockers of $nNa_v1.5$-dependent inward currents in whole-cell patch-clamp experiments in MDA-MB-231 cells. The identified lead compounds **1** and **4** inhibited peak sodium currents in MDA-MB-231 cells by 35 % and 25 % respectively at 1 μM. These two compounds also produced 30 % reduction of the invasion of MDA-MB-231 cells at 1 μM without affecting the cell viability. The lead compounds are very effective in inhibiting cell invasion producing an effect similar to what is observed for TTX at a much lower concentration. Our lead compounds are much more drug-like and have simpler chemical structures compared to TTX. In addition, our lead compounds are more active in inhibiting breast cancer cell invasion than the known VGSC-blocking drugs such as ranolazine and phenytoin. Compounds **1** and **4**, unlike ranolazine and phenytoin, are developed to specifically target the $nNa_v1.5$ and represent new and more potent class of compounds that may be further developed in to drugs for the treatment of breast cancer metastasis.

4. Experimental Procedures

4.1. Cell viability assay: Cytotoxicity of the compounds was tested in a MTS assay. Cells were seeded in 96 well plates at 10^4 cells/well in growth media (5 % FBS in DMEM) and

incubated for 24 h at 37 ^{o}C in 5 % CO_2. Various concentrations of test compounds (1, 5, 10 and 25 μM) or vehicle control (0.25 % DMSO in PBS) were added and the cells were incubated for an additional 24 h. For each test concentration, 5 wells were allotted. After 24 h of incubation proliferation was determined using MTS. 20 μL of MTS were added to each well and the cells were incubated for an additional 30 min. UV absorbance was recorded at 490 nm. The cytotoxicity of the test compounds was compared to the vehicle control (0.25 % DMSO in PBS) and results were compiled as the mean of five repeats using the GraphPad Prism software.

4.2. Cell invasion inhibition assay: Cell invasion experiments were carried out in 24 well plates containing BD Matrigel® invasion chambers (BD Biosciences). The invasion chambers were hydrated for 2 h in the incubator at 37 ^{o}C with 200 μL (5 % FBS in DMEM) in the upper insert and 800 μL (10 % FBS in DMEM) in the lower well that acted as a chemoattractant. MDA-MB-231 cells (4×10^4) were seeded in the upper chamber. Various concentrations of the test compounds (0.1 and 1 μM) or vehicle control (0.2% DMSO in PBS) were added in both the lower and upper chambers to maintain uniformity of concentration by 1:100 dilutions. After incubating the cells for 24 h at 37 ^{o}C, under 5 % CO_2, invaded cells were fixed and stained using a Hema kit. The migrated cells were counted under the microscope by selecting five regions on the whole membrane. Results were compiled as a mean of three repeats using graphPad Prism software. The results are given as a mean ± SD.

4.3. Electrophysiology: A whole cell patch clamp technique was used for recording the sodium channel activity in MDA-MB-231 cells. 30,000 cells were seeded into a 35 mm petri dish with the growth media (5% FBS in DMEM). Na^+ currents were recorded under voltage-

clamp mode using an Axopatch 200B patch clamp amplifier (Axon Instruments, USA), compensating for cell capacitance and series resistance by 60 %. The P/2 sub pulse protocol was applied to correct the linear component of capacitance and cell leak. Borosilicate glass was used to pull the patch pipettes at a resistance of 3-5 MΩ. Analog signals were filtered at 5 kHz and sampled at 10 kHz via a 1440A Digidata converter and analyzed using pCLAMP software (v10.4, Axon Instruments). Cells were studied in ruptured, whole-cell, voltage-clamp mode of the patch-clamp technique. Before starting the experiment growth medium was removed and replaced with physiological saline solution (PSS, composition given below). In this experiment the tip of the micro capillary (perifusion system) delivering the PSS or the test compound was placed almost on top of the cell, so that the cells were continuously perifused with the respective solutions. The stock solution for test compounds was prepared at 10 mM in 100% DMSO and the test concentration used in the assay was 1 μM and 10 μM (0.2 % DSMO in PSS). Sodium currents were recorded by depolarizing the cells from a holding potential of -100 mV to a maximal test pulse of -5 mV for 30 ms every 500 ms. The protocol used to build the current-voltage (I_{Na}-V) curve was as follows. From a holding potential of -100 mV, the membrane was stepped to a potential of +60 mV, with 5 mV increments, for 50 ms at a frequency of 2 Hz. The physiological saline solution (PSS) contained (in mM): NaCl 140, KCl 4, $MgCl_2$ 1, $CaCl_2$ 2, NaH_2PO_4 0.33, D-Glucose 11.1, and HEPES 10, and was adjusted to pH 7.4. The intrapipette solution (in mM) contained: KCl 130, NaCl 15, $CaCl_2$ 0.37, $MgCl_2$ 1, Mg-ATP 1, EGTA 1, and HEPES 10, and was adjusted to pH 7.2.

4.4. General Methods for Synthesis: Solvent evaporations were carried out *in vacuo* using a rotary evaporator. Thin layer chromatography (TLC) was performed on silica gel plates with

fluorescent indicator (Dynamic Adsorbents, Inc., Aluminum backed TLC, 20 X 20 cm F-254, 200 µm). Spots were visualized by UV light (254 and 365 nm) or staining agents such as ninhydrin, $KMnO_4$ and iodine. Purification by column and flash chromatography was carried out using silica gel (32-63 µm) from Dynamic Absorbent in the solvent systems indicated. The amount (weight) of silica gel for column chromatography was in the range of 50-100 times the amount (weight) of the crude compounds being separated. The NMR spectra were recorded on a Bruker DPX 300 spectrometer. Chemical shifts are reported in ppm relative to TMS or $CDCl_3$ as internal standard. The values of chemical shifts (δ) and coupling constants J were given in parts per million and in Hz, respectively. Mass spectra were recorded on a MicroMass Platform LCC instrument. HRMS were obtained on a Waters AutoSpec-UltimaTM NT mass spectrometer with an EI source. Anhydrous solvents used for reactions were purchased in Sure-Seal^{TM} bottles from Aldrich chemical company. THF was freshly distilled over sodium/benzophenone. Other reagents were purchased from Aldrich, Alfa Aesar or Acros and used as received.

4.5. Synthesis of compounds 1-3, General procedure: To a solution of alkyl amine (1 equiv) in DMSO (10mL), a solution of alkyl chloride (1 equiv.) in DMSO (5 mL) and Et_3N (1 equiv.) were added. The reaction mixture was heated at 80-90^{o}C under a N_2 atmosphere for 8 h. TLC examination (MeOH / NH_3 saturated CH_2Cl_2, 1:19) indicated the completion of the reaction. The reaction mixture was diluted with EtOAc (60mL), washed with 1N NaOH (3 × 20 mL), water (2 × 20 mL), brine (20 mL) and dried over Na_2SO_4. The drying agent was filtered off and the filtrate was concentrated under vacuum to obtain the crude product which was purified by column chromatography over Si gel using MeOH/ NH_3 saturated CH_2Cl_2 (1:49) to obtain pure compounds **1-3** in 58 – 60 % yield.

4,4-Bis(4-fluorophenyl)-*N*-(3-(piperdin-1-yl)propyl)butan-1-amine (1): Prepared from 3-(*N*-piperidino)propylamine (2.50 g, 17.6 mmol) and 4,4-di-(4-fluorophenyl)butyl chloride **6** (4.93 g, 17.6 mmol) to afford compound **1** (4.00 g, 60%) as a liquid ($MeOH/NH_3$ saturated CH_2Cl_2, 1:19, Rf = 0.40). ^{1}H-NMR ($CDCl_3$) δ 1.34 – 1.46 (m, 4H), 1.52 (quint, 4H, *J* = 5.3 Hz), 1.65 (quint, 2H, *J* = 7.5 Hz), 2.01 (q, 2H, *J* = 8 Hz), 2.20 – 2.42 (m, 8H), 2.60 (t, 4H, *J* = 7.5 Hz), 3.85 (t, 1H, *J* = 7.5 Hz), 6.89 – 6.99 (m, 4H), 7.10 – 7.19 (m, 4H); ^{13}C-NMR ($CDCl_3$) δ 24.4, 26.0, 27.0, 28.5, 33.7, 49.0, 49.7, 49.8, 54.7, 57.9, 115.1 (115.4, F- coupling), 129.0 (129.1, F- coupling), 140.5 (140.6, F- coupling), 159.7 (162.9, F- coupling); MS (ES+) m/z 387 (M+H); HRMS measured for $C_{24}H_{32}F_2N_2$: $[M+H]^+$ 386.2535 (found), 386.2534 (calc).

4,4-Bis(4-fluorophenyl)-*N*-(3-phenylpropyl)butan-1-amine (2): Prepared from 3-phenylpropylamine (0.240 g, 1.78 mmol), and 4,4-di-(4-fluorophenyl)butyl chloride, **6** (0.500 g, 1.78 mmol) to afford compound **2** (0.230 g, 60.6%) as a thick liquid ($MeOH/NH_3$ saturated CH_2Cl_2, 1:19, Rf = 0.50). ^{1}H-NMR ($CDCl_3$) δ 1.47 (quint, 3H, *J* = 7.5 Hz), 1.84 (t, 2H, *J* = 7.5 Hz), 1.98 (q, 2H, *J* = 7.8 Hz), 2.63 (quint, 6H, *J* = 7.1 Hz), 3.82 (t, 1H, *J* = 7.8 Hz), 3.92 (bs, 1H), 6.90 – 7.10 (m, 4H), 7.08 – 7.21 (m, 7H), 7.22 – 7.30 (m, 2H); ^{13}C-NMR ($CDCl_3$) δ 27.6, 30.7, 33.5 (2C), 49.0, 49.3, 49.7, 115.3, 115.6, 126.1, 128.5, 128.6, 129.2, 129.3, 140.43, 140.5, 141.6, 159.9, 163.1; MS (ES+) m/z 380 (M+H); HRMS measured for $C_{25}H_{27}F_2N$: $[M+H]^+$ 379.2116 (found), 379.2112 (calc).

4,4-Bis(4-fluorophenyl)-*N*-phenylethylbutan-1-amine (3): Prepared from 2-phenylethylamine (0.996 g, 8.22 mmol) and 4,4-di-(4-fluorophenyl)butyl chloride **1** (2.31 g, 8.22 mmol) to afford compound **3** (1.74 g, 58.0%) as a liquid (40% ethyl acetate / 55% hexanes / 5% Et_3N, Rf = 0.35). ^{1}H-NMR ($CDCl_3$) δ 1.37 -1 .44 (m, 2H), 1.63 (bs, 1H), 1.97 (t, 2H, *J* = 7.4 Hz), 2.59 – 2.65 (m, 2H), 2.78 (t, 2H, *J* = 7.0 Hz), 2.83 (q, 2H, *J* = 7.7 Hz), 3.82 (q, 1H, *J* = 8.2 Hz), 6.90 – 6.97 (m,

4H), 7.09 – 7.21 (m, 7H), 7.22 – 7.29 (m, 2H); ^{13}C-NMR ($CDCl_3$) δ 28.5, 33.8, 36.4, 49.8, 49.9, 51.2, 115.4 (115.5, F-coupling), 126.4, 128.7, 128.9, 129.2, 129.3, 140.1 (140.7, F-coupling), 160.8 (162.2, F-coupling); MS (ES+) m/z 366 (M+H); HRMS measured for $C_{24}H_{25}F_2N$: $[M+H]^+$ 365.1954 (found), 365.1955 (calc).

4-(4-Fluorophenyl) butan-1-ol (8): A suspension of $AlCl_3$ (4.00 g, 30.0 mmol) in anhydrous CH_2Cl_2 (100 mL) was stirred under a N_2 atmosphere at 0 ^oC for 10 min followed by the addition of borane tert-butylamine complex (5.20 g, 60.0 mmol). The reaction mixture was allowed to stir at 0 ^oC till it gave a clear solution (10-15 mins). To the clear reaction mixture a solution of 4-(4-fluorophenyl)-4-oxobutanoic acid **7** (2.00 g, 10 mmol) in anhydrous CH_2Cl_2 (10 mL) was added. The resulting mixture was stirred at 0^oC for 2h, and TLC examination (EtOAc/hexanes, 1:4, Rf = 0.30) indicated completion of the reaction. The reaction mixture was quenched by the addition of 0.1 N HCl (50 mL). It was extracted with EtOAc (3 × 50 mL); the combined organic layer was washed with 0.1 N HCl (2 × 50 mL), brine (50 mL), and dried over Na_2SO_4. The drying agent was filtered off and the filtrate was concentrated under vacuum to obtain the crude product. The crude product was purified by column chromatography over Si gel using EtOAc / hexanes (1:4) to afford 4-(4-fluorophenyl)butan-1-ol 4 (0.880 g, 52.3% yield) as a colorless liquid. ^{1}H-NMR ($CDCl_3$) δ 1.56 – 1.73 (m, 4H), 2.14 (bs, 1H), 2.61 (t, 2H, *J* = 7.4 Hz), 3.65 (t, 2H, *J* = 6.3 Hz), 6.91- 7.00 (m, 2H), 7.08 – 7.16 (m, 2H); ^{13}C-NMR ($CDCl_3$) δ 27.9, 32.3, 35.0, 62.9, 115.0 (115.3), 129.8 (129.9), 138.0 (138.1), 159.8 (163.0).

4-(4-Fluorophenyl)butan-1-al (9): PCC (7.13 g, 33.1 mmol) was ground with silica gel (7.13 g) and suspended in anhydrous CH_2Cl_2 (100 mL) under a N_2 atmosphere at room temperature. After stirring for 10-15 mins, a solution of 4-(4-fluorophenyl)butan-1-ol (**8)** (0.857 g, 5.09 mmol) in anhydrous CH_2Cl_2 (10 mL) was added to the suspension. After 6 h of stirring at room

temperature, TLC examination (EtOAc/hexanes, 1:4, Rf = 0.50) indicated completion of the reaction. The reaction mixture was filtered through celite and washed with CH_2Cl_2 (200 mL). The filtrate was concentrated under vacuum to obtain the crude product. The crude product was purified by column chromatography over silica gel, using EtOAc / hexanes (1:4) to afford 4-(4-fluorophenyl)butan-1-al (**9**) (0.444 g, 52.5% yield) as a colorless liquid. ^{1}H-NMR ($CDCl_3$) δ 1.92 (pent, 2H, J = 7.7 Hz), 2.44 (td, 2H, J_1 = 7.2 Hz, J_2 = 1.5 Hz), 2.62 (t, 2H, J = 7.7 Hz), 6.91 – 7.01 (m, 2H), 7.08 – 7.16 (m, 2H), 9.74 (t, 1H, J = 1.5 Hz); ^{13}C-NMR ($CDCl_3$) δ 23.9, 34.3, 43.1, 115.1 (115.4, F-coupling), 129.9, 137.0, 159.9 (163.1, F-coupling), 202.2.

4-(4-Fluorophenyl)-N-(3-(piperdin-1-yl)propyl)butan-1-amine (4): 3-(*N*-Piperidino)propyl amine (0.380 g, 2.67 mmol) was dissolved in anhydrous CH_2Cl_2 (25 mL) under a N_2 atmosphere. 4-(4-Fluorophenyl)butan-1-al (**9)** (0.444 g, 2.67 mmol) was added to the reaction mixture. After stirring the reaction mixture for 30 mins, $NaBH(OAc)_3$ (1.13 g, 5.34 mmol) was added. After stirring the reaction mixture for 5 h at room temperature, TLC examination (MeOH/NH_3 saturated CH_2Cl_2, 1:19, Rf = 0.40) indicated completion of the reaction. The reaction mixture was concentrated under vacuum and taken up into EtOAc (60 mL); the organic layer was washed with 1 N NaOH (3 × 30 mL), water (30 mL), brine (30 mL) and dried over Na_2SO_4. The drying agent was filtered off and the filtrate was concentrated under vacuum to obtain the crude product. The crude product was purified by column chromatography over Si gel, using MeOH/NH_3 saturated CH_2Cl_2 (3:97) to afford 4-(4-fluorophenyl)-*N*-(3-(piperdin-1-yl)propyl)butan-1-amine (**4)** (0.224 g, 30.0% yield). ^{1}H-NMR ($CDCl_3$) δ 1.35 - 1.45 (m, 2H), 1.46 - 1.61 (m, 7H), 1.62 - 1.73 (m, 3H), 2.27 - 2.43 (m, 6H), 2.60 (quint, 6H, J = 7.4 Hz), 6.89 - 6.98 (m, 2H), 7.06 - 7.14 (m, 2H); ^{13}C-NMR ($CDCl_3$) δ 24.6, 26.2, 27.0, 29.5, 29.7, 35.1, 49.2, 49.9, 54.8, 58.1, 115.0 (115.2, F-coupling), 129.8 (129.9, F-coupling), 138.1 (138.2, F-coupling), 159.7 (163.0, F-

coupling); MS (ES+) m/z 293 (M+H); HRMS measured for C18H29FN2: [M+H]+ 292.2324 (found), 292.2315 (calc).

Neopentyl magnesium bromide (11): In an oven dried three-neck flask connected to a condenser and dropping funnel was placed dry magnesium turnings (1.60 g, 66.0 mmol) under a N_2 atmosphere. The magnesium was further flame dried for half an hour under N_2 before adding a crystal of I_2 and anhydrous THF (20 mL). A solution of neopentyl bromide **10** (10.0 g, 66.0 mmol) in THF (20 mL) was slowly added to the reaction mixture through a dropping funnel. Disappearance of the coloration and beginning of effervescence indicated the onset of the reaction. No external heating was applied until the complete addition of neopentyl bromide. After refluxing for 3 h, the heating was stopped and the concentration of Grignard reagent generated was determined to be 1.48 M by titration against a solution of isopropanol in xylene. This Grignard reagent was used in the next step.

((5,5-Dimethylhex-1-en-1-yl)oxy)trimethylsilane (12): 1.48 M Neopentyl magnesium bromide (**7**) (40 mL) was dissolved in anhydrous THF (150 mL) and was cooled to -100 ^oC followed by the addition of $CuBr.Me_2S$ (0.510 g, 2.50 mmol) and HMPA (21.1 g, 118 mmol) under a N_2 atmosphere. After stirring for 10 mins, a solution of acrolein (2.76 g, 49.2 mmol) and chlorotrimethylsilane (10.7 g, 98.4 mmol) in THF (50 mL) were added to the reaction mixture via a cannula. After stirring the reaction mixture for 4 h at -100 ^oC under a N_2 atmosphere, Et_3N (9.95 g, 98.4 mmol) and silica gel (30.0 g, 4 times the expected weight of the product) was added. After stirring for 10 min at room temperature, hexanes (400 mL) was added. The slurry was filtered off and the filtrate was concentrated under vacuum to obtain the crude product. The crude product was purified by vacuum distillation (5 T, 66 ^oC) and (5,5-dimethylhex-1-enyloxy)trimethylsilane (**12)** (6.00 g, 61.0%) was obtained as colorless liquid (hexanes, Rf =

0.50); ^{1}H-NMR ($CDCl_3$) δ 0.16 (s, 9H), 0.86 (s, 9H), 1.14 – 1.23 (m, 2H), 1.78 – 1.88 (m, 2H), 4.96 (dt, 1H, J_1 = 12Hz, J_2 = 7.4 Hz), 6.18 (dt, J_1 = 12 Hz, J_2 = 1.2 Hz); ^{13}C-NMR ($CDCl_3$) δ 0.2, 22.9, 29.6, 30.4, 45.3, 113.0, 139.2.

5,5-Dimethyl-*N*-(3-(piperidin-1-yl)propyl)hexan-1-amine (5): Compound **12** (0.782 g, 3.97 mmol) was dissolved in anhydrous MeOH (15 mL) under a N_2 atmosphere. The reaction mixture was cooled to 0 ^{o}C and KF (0.396 g, 6.82 mmol) was added. After stirring the reaction mixture for 15 min, TLC examination (EtOAc/hexanes, 1:19, Rf = 0.60) indicated a complete conversion to 5,5-dimethylhexanal (**13)**, which was directly added via cannula to the solution of 3-(*N*-piperidino)propylamine (0.566 g, 3.97 mmol) in anhydrous MeOH (70 mL) under a N_2 atmosphere. After stirring the reaction mixture for 30 min, $NaBH(OAc)_3$ (1.68 g, 7.94 mmol) was added to the reaction mixture. After 5 h of stirring at room temperature, TLC examination (MeOH/NH_3 saturated CH_2Cl_2, 1:19, Rf = 0.40) indicated the completion of reaction. The reaction mixture was concentrated under vacuum, the residue taken up in EtOAc (50 mL) and washed with 1 N NaOH (3 × 30 mL). The organic layer was washed with water (30 mL) followed by brine (30mL) and dried over Na_2SO_4. The drying agent was filtered off and the filtrate was concentrated under vacuum to obtain the crude product. The crude product was purified by column chromatography over silica gel using MeOH / NH_3 saturated CH_2Cl_2 (3:97) to afford 5,5-dimethyl-*N*-(3-(piperidin-1-yl)propyl)hexan-1-amine (**5)** (0.500 g, 49.5%) as a clear light yellow liquid. ^{1}H-NMR ($CDCl_3$) δ 0.84 (s, 9H), 1.10 – 1.31 (m, 4H), 1.35 – 1.49 (m, 4H), 1.55 (quint, 4H, J = 5.4 Hz), 1.68 (quint, 2H, J = 7.2 Hz), 2.27 – 2.39 (m, 6H), 2.53 – 2.65 (m, 4H); ^{13}C-NMR ($CDCl_3$) δ 22.6, 24.7, 26.2, 27.3, 29.6, 30.5, 31.3, 44.4, 49.2, 50.3, 54.9, 58; HRMS measured for $C_{16}H_{34}N_2$: [M+H]+ 254.2731 (found), 254.2722 (calc).

5. Acknowledgements

Funding from NIH (1UL1RR025777, R03DE025058-0) is acknowledged. The authors wish to acknowledge the financial support by the Collaborative Programmatic Development Grant from the UAB Comprehensive Cancer Center. SD would like to acknowledge the graduate fellowship from the UAB chemistry department. SR was supported by the INSERM, the Région Centre-Val de Loire, the "Ligue Nationale contre le Cancer", the "Association CANCEN", and the "Prix Ruban Rose Avenir 2017".

References

1. DeSantis, C. E.; Ma, J.; Goding Sauer, A.; Newman, L. A.; Jemal, A., Breast cancer statistics, 2017, racial disparity in mortality by state. *CA Cancer J Clin* **2017,** *67* (6), 439-448.
2. Siegel, R. L.; Miller, K. D.; Jemal, A., Cancer statistics, 2018. *CA Cancer J Clin* **2018,** *68* (1), 7-30.
3. Chaffer, C. L.; Weinberg, R. A., A perspective on cancer cell metastasis. *Science* **2011,** *331* (6024), 1559-64.
4. Weigelt, B.; Peterse, J. L.; van 't Veer, L. J., Breast cancer metastasis: markers and models. *Nat. Rev.. Cancer* **2005,** *5* (8), 591-602.
5. Guan, X., Cancer metastases: challenges and opportunities. *Acta Pharmaceutica Sinica B* **2015,** *5* (5), 402-418.
6. Mehlen, P.; Puisieux, A., Metastasis: a question of life or death. *Nat. Rev.. Cancer* **2006,** *6* (6), 449-58.
7. Hanahan, D.; Weinberg, R. A., The hallmarks of cancer. *Cell* **2000,** *100* (1), 57-70.

8. Weber, G. F., Why does cancer therapy lack effective anti-metastasis drugs? *Cancer Lett* **2013,** *328* (2), 207-11.

9. Chambers, A. F.; Groom, A. C.; MacDonald, I. C., Dissemination and growth of cancer cells in metastatic sites. *Nat. Rev. Cancer* **2002,** *2*, 563.

10. Roger, S.; Potier, M.; Vandier, C.; Besson, P.; Le Guennec, J. Y., Voltage-gated sodium channels: new targets in cancer therapy? *Curr Pharm Des* **2006,** *12* (28), 3681-95.

11. Brackenbury, W. J., Voltage-gated sodium channels and metastatic disease. *Channels (Austin)* **2012,** *6* (5), 352-61.

12. Lastraioli, E.; Iorio, J.; Arcangeli, A., Ion channel expression as promising cancer biomarker. *Biochim. Biophys. Acta* **2015,** *1848* (10 Pt B), 2685-702.

13. Chahine, M.; Desaphy, J. F., Editorial: Recent Advances in Voltage-Gated Sodium Channels, their Pharmacology and Related Diseases. *Front Pharmacol* **2016,** *7*, 20.

14. Patel, F.; Brackenbury, W. J., Dual roles of voltage-gated sodium channels in development and cancer. *Int J Dev Biol* **2015,** *59* (7-9), 357-66.

15. Besson, P.; Driffort, V.; Bon, E.; Gradek, F.; Chevalier, S.; Roger, S., How do voltage-gated sodium channels enhance migration and invasiveness in cancer cells? *Biochim. Biophys. Acta* **2015,** *1848* (10 Pt B), 2493-501.

16. Catterall, W. A., Voltage-gated sodium channels at 60: structure, function and pathophysiology. *J Physiol* **2012,** *590* (11), 2577-89.

17. Roger, S.; Gillet, L.; Le Guennec, J. Y.; Besson, P., Voltage-gated sodium channels and cancer: is excitability their primary role? *Front Pharmacol* **2015,** *6*, 152.

18. House, C. D.; Vaske, C. J.; Schwartz, A. M.; Obias, V.; Frank, B.; Luu, T.; Sarvazyan, N.; Irby, R.; Strausberg, R. L.; Hales, T. G.; Stuart, J. M.; Lee, N. H., Voltage-gated Na+

channel SCN5A is a key regulator of a gene transcriptional network that controls colon cancer invasion. *Cancer Res.* **2010,** *70* (17), 6957-67.

19. Blandino, J. K.; Viglione, M. P.; Bradley, W. A.; Oie, H. K.; Kim, Y. I., Voltage-dependent sodium channels in human small-cell lung cancer cells: role in action potentials and inhibition by Lambert-Eaton syndrome IgG. *J. Membr. Biol.* **1995,** *143* (2), 153-63.

20. Grimes, J. A.; Fraser, S. P.; Stephens, G. J.; Downing, J. E.; Laniado, M. E.; Foster, C. S.; Abel, P. D.; Djamgoz, M. B., Differential expression of voltage-activated Na+ currents in two prostatic tumour cell lines: contribution to invasiveness in vitro. *FEBS letters* **1995,** *369* (2-3), 290-4.

21. Yamashita, N.; Hamada, H.; Tsuruo, T.; Ogata, E., Enhancement of voltage-gated Na+ channel current associated with multidrug resistance in human leukemia cells. *Cancer Res.* **1987,** *47* (14), 3736-41.

22. Roger, S.; Besson, P.; Le Guennec, J. Y., Involvement of a novel fast inward sodium current in the invasion capacity of a breast cancer cell line. *Biochim. Biophys Acta* **2003,** *1616* (2), 107-11.

23. Brackenbury, W. J.; Chioni, A. M.; Diss, J. K.; Djamgoz, M. B., The neonatal splice variant of Nav1.5 potentiates in vitro invasive behaviour of MDA-MB-231 human breast cancer cells. *Breast Cancer Res and Trea* **2007,** *101* (2), 149-60.

24. Catterall, W. A., From ionic currents to molecular mechanisms: the structure and function of voltage-gated sodium channels. *Neuron* **2000,** *26*, 13-25

25. Catterall, W. A.; Goldin, A. L.; Waxman, S. G., International Union of Pharmacology. XLVII. Nomenclature and structure-function relationships of voltage-gated sodium channels. *Pharmacol Rev* **2005,** *57* (4), 397-409.

26. Fraser, S. P.; Diss, J. K.; Chioni, A. M.; Mycielska, M. E.; Pan, H.; Yamaci, R. F.; Pani, F.; Siwy, Z.; Krasowska, M.; Grzywna, Z.; Brackenbury, W. J.; Theodorou, D.; Koyuturk, M.; Kaya, H.; Battaloglu, E.; De Bella, M. T.; Slade, M. J.; Tolhurst, R.; Palmieri, C.; Jiang, J.; Latchman, D. S.; Coombes, R. C.; Djamgoz, M. B., Voltage-gated sodium channel expression and potentiation of human breast cancer metastasis. *Clin Cancer Res* **2005,** *11* (15), 5381-89.

27. Gillet, L.; Roger, S.; Besson, P.; Lecaille, F.; Gore, J.; Bougnoux, P.; Lalmanach, G.; Le Guennec, J. Y., Voltage-gated Sodium Channel Activity Promotes Cysteine Cathepsin-dependent Invasiveness and Colony Growth of Human Cancer Cells. *J. Biol. Chem.* **2009,** *284* (13), 8680-91.

28. Brisson, L.; Gillet, L.; Calaghan, S.; Besson, P.; Le Guennec, J. Y.; Roger, S.; Gore, J., Na(V)1.5 enhances breast cancer cell invasiveness by increasing NHE1-dependent H(+) efflux in caveolae. *Oncogene* **2011,** *30* (17), 2070-6.

29. Bon, E.; Driffort, V.; Gradek, F.; Martinez-Caceres, C.; Anchelin, M.; Pelegrin, P.; Cayuela, M. L.; Marionneau-Lambot, S.; Oullier, T.; Guibon, R.; Fromont, G.; Gutierrez-Pajares, J. L.; Domingo, I.; Piver, E.; Moreau, A.; Burlaud-Gaillard, J.; Frank, P. G.; Chevalier, S.; Besson, P.; Roger, S., SCN4B acts as a metastasis-suppressor gene preventing hyperactivation of cell migration in breast cancer. *Nat Commun* **2016,** *7*, 13648.

30. Gupta, G. P.; Massague, J., Cancer metastasis: building a framework. *Cell* **2006,** *127* (4), 679-95.

31. Mohamed, M. M.; Sloane, B. F., Cysteine cathepsins: multifunctional enzymes in cancer. *Nat. Rev. Cancer* **2006,** *6* (10), 764-75.

32. Egeblad, M.; Werb, Z., New functions for the matrix metalloproteinases in cancer progression. *Nat. Rev. Cancer* **2002,** *2* (3), 161-74.

33. Busco, G.; Cardone, R. A.; Greco, M. R.; Bellizzi, A.; Colella, M.; Antelmi, E.; Mancini, M. T.; Dell'Aquila, M. E.; Casavola, V.; Paradiso, A.; Reshkin, S. J., NHE1 promotes invadopodial ECM proteolysis through acidification of the peri-invadopodial space. *FASEB journal : official publication of the Federation of American Societies for Experimental Biology* **2010,** *24* (10), 3903-15.

34. Nelson, M.; Yang, M.; Millican-Slater, R.; Brackenbury, W. J., Nav1.5 regulates breast tumor growth and metastatic dissemination in vivo. *Oncotarget* **2015,** *6* (32), 32914-29.

35. Camerino, D. C.; Desaphy, J. F.; Tricarico, D.; Pierno, S.; Liantonio, A., Therapeutic approaches to ion channel diseases. *Adv Genet* **2008,** *64*, 81-145.

36. Fozzard, H. A.; Sheets, M. F.; Hanck, D. A., The sodium channel as a target for local anesthetic drugs. *Front Pharmacol* **2011,** *2*, 68.

37. Zha, C.; Brown, G. B.; Brouillette, W. J., A highly predictive 3D-QSAR model for binding to the voltage-gated sodium channel: design of potent new ligands. *Bioorganic Med. Chem.* **2014,** *22* (1), 95-104.

38. Cramer III, R. D.; Patterson, D. E.; Bunce, J. D., Comparative molecular field analysis (CoMFA) 1. Effect of shape on binding of steroids to carrier proteins. *J. Am. Chem. Soc.* **1988,** *110*, 5959-67.

39. Lau, C. K. D., C.; Scheigetz, J.;, Reductive deoxygenation of aryl aldehydes and ketones by tert-butylamine-borane and aluminium chloride. *J. Org. Chem.* **1989,** *54*, 491-494.

40. Satoshi Matsuzawa, Y. H., Eiichi Nakamura, Isao Kuwajima, Chlorosilane-accelerated conjugate addition of catalytic and stoichiometric organocopper reagents. *Tetrahedron* **1989,** *45* (2), 349-362.

41. Welch, D. R.; Krizman, D. B.; Nicolson, G. L., Multiple phenotypic divergence of mammary adenocarcinoma cell clones. I. In vitro and in vivo properties. *Clin. Exp. Metastasis* **1984,** *2* (4), 333-55.

42. Driffort, V.; Gillet, L.; Bon, E.; Marionneau-Lambot, S.; Oullier, T.; Joulin, V.; Collin, C.; Pages, J. C.; Jourdan, M. L.; Chevalier, S.; Bougnoux, P.; Le Guennec, J. Y.; Besson, P.; Roger, S., Ranolazine inhibits NaV1.5-mediated breast cancer cell invasiveness and lung colonization. *Mol. Cancer* **2014,** *13*, 264.

43. Nelson, M.; Yang, M.; Dowle, A. A.; Thomas, J. R.; Brackenbury, W. J., The sodium channel-blocking antiepileptic drug phenytoin inhibits breast tumour growth and metastasis. *Mol. Cancer* **2015,** *14*, 13.

44. Yang, M.; Kozminski, D. J.; Wold, L. A.; Modak, R.; Calhoun, J. D.; Isom, L. L.; Brackenbury, W. J., Therapeutic potential for phenytoin: targeting Na(v)1.5 sodium channels to reduce migration and invasion in metastatic breast cancer. *Breast Cancer Res. Treat.* **2012,** *134* (2), 603-15.

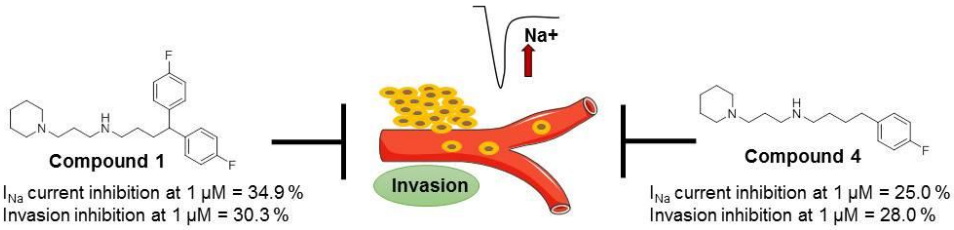

Highlights

- Identified novel nNav1.5 blockers that inhibit breast cancer cell invasion.
- Most active compound blocked nNav1.5 currents by 50% at 1 μM.
- Most active compound displayed 30% reduction in cell invasion at 0.1 μM.